http://dx.doi.org/10.5012/bkcs.2011.32.10.3571

Morphology Control of Single Crystalline Rutile TiO_2 Nanowires

Yi-Seul Park and Jin Seok Lee*

*Department of Chemistry, Sookmyung Women's University, Seoul 140-742, Korea. *E-mail: jinslee@sookmyung.ac.kr*
Received July 7, 2011, Accepted August 3, 2011

Nano-scaled metal oxides have been attractive materials for sensors, photocatalysis, and dye-sensitization for solar cells. We report the controlled synthesis and characterization of single crystalline TiO_2 nanowires via a catalyst-assisted vapor-liquid-solid (VLS) and vapor-solid (VS) growth mechanism during TiO powder evaporation. Scanning electron microscope (SEM) and transmission electron microscope (TEM) studies show that as grown TiO_2 materials are one-dimensional (1D) nano-structures with a single crystalline rutile phase. Also, energy-dispersive X-ray (EDX) spectroscopy indicates the presence of both Ti and O with a Ti/O atomic ratio of 1 to 2. Various morphologies of single crystalline TiO_2 nano-structures are realized by controlling the growth temperature and flow rate of carrier gas. Large amount of reactant evaporated at high temperature and high flow rate is crucial to the morphology change of TiO_2 nanowire.

Key Words : TiO_2, Nanowire, Morphology, Vapor-liquid-solid mechanism

Introduction

Titanium dioxide (TiO_2) nano-structures such as nanotubes,[1] nanowires,[2] nanowhiskers,[3] nanorods,[4] nanobelts,[5] and nanofibers[6] have been recently studied by many researchers because of its wide range of applications in gas sensors,[7] photocatalysis,[8,9] dye-sensitization for solar cells,[10,11] and solar water splitting for hydrogen production.[12-14] They could be synthesized to single crystalline TiO_2 with different crystal phase, such as anatase, brookite, and rutile. Among the three naturally crystalline TiO_2 phases, rutile TiO_2 usually forms relatively bulky structures with a poorly controlled morphology and low surface area because it is the most thermodynamically stable.

Over the past decade, one-dimensional (1D) nano-structured materials have emerged as promising materials for fundamental studies and possible technological application.[15] These structures exhibit physical and chemical properties distinct from their bulk counterparts due to radial confinement, while they retain the advantages of wirelike connectivity. Among them, TiO_2 nanowire as 1D nano-structure particularly attracted much interest because of the unique properties depending on their size.[16,17]

TiO_2 nanowire is typically achieved using either of the two different synthetic methods developed over the past few years: one is 'wet-chemistry' method such as electrochemical,[18] sol-gel electrophoresis,[19] hydrothermal,[20,21] and solvothermal method,[22] and the other is 'dry' method including thermal evaporation[23-25] and metal-organic chemical vapor deposition (MOCVD).[26-28] But, the TiO_2 nanowires produced by above 'wet-chemistry' method have difficult integrating into device fabrication due to poor cystallinity. Also, they need to handle the additional processes in order to improve their crystallinity which were accompanied the complexity of the processes.

Here, we synthesized the single crystalline TiO_2 nano-structures with rutile phase using chemical vapor deposition (CVD) technique[29,30] as 'dry' method. We also controlled the morphology of TiO_2 nano-structures, such as nanowire and nanobelt, by changing reaction conditions such as growth temperature and flow rate of carrier gas. It is important to control the morphology of TiO_2 nanowires[31,32] because we can adjust their optical and electrical properties by changing the shapes of nano-structures.

Experimental Section

Materials. TiO (−325 mesh, 99.9%) powder was purchased from Aldrich. Isopropyl alcohol was purchased from Duksan. SiO_2/Si wafers were purchased from University Wafer.

Preparation of Metal Covered Substrate as a Catalyst. Silicon (Si) wafers with 200 nm thick thermally grown SiO_2 (University Wafer) were coated with 50 nm thick Ti and then 2 nm thick Ni which are used as catalyst were covered on the Ti layer by thermal evaporation. They were cut into small pieces with the specific size of 5 mm (width) × 5 mm (length). These Ni/Ti/SiO_2/Si substrates were ultrasonically cleaned using isopropyl alcohol using an ultrasound cleaning bath equipped with two 100-W ultrasound generators operated at 28 kHz (Saehan Ultrasonic SH-2100).

Measurements. The scanning electron microscope (SEM) images of the TiO_2 nano-structures were obtained from a FE-SEM (Hitachi S-4300) at an acceleration voltage of 10 to 20 kV, which was performed on the as-synthesized product on substrates. A platinum/palladium alloy (in the ratio of 8 to 2) was deposited with a thickness of about 15 nm on top of the samples. And their single crystalline structure was analyzed with a JEOL 2010 transmission electron microscope (TEM) with energy-dispersive X-ray (EDX) mapping capabilities. Samples for TEM imaging were made by depositing a hexane solution of nanowires (prepared by soni-

cation of as-synthesized substrate in hexane) onto holey carbon 300 mesh copper grids (Structure Probe, Inc.). The X-ray diffraction patterns for the identification of produced nanowires were obtained from a Rigaku diffractometer (D/MAX-1C) with the monochromatic beam of Cu Kα.

Result and Discussion

Synthesis and Characterization of TiO_2 Nanowires. We synthesized the high single crystalline TiO_2 nanowires using chemical vapor deposition (CVD) method, as shown in Figure 1(a). Titanium oxide (TiO) powder as a precursor for TiO_2 crystal growth was located at the center of the 8 cm quartz boat and then Ni/Ti/SiO_2/Si substrate was loaded next to the TiO powder in the quartz boat. Then, quartz boat was placed at the center of the heating zone in a tube furnace (Lindberg/Blue M, 12 in. length) equipped with a 1 in. diameter quartz tube. Before the experiment, the quartz tube was evacuated to below 0.1 torr and flushed several times with high purity Ar gas (99.999%) to minimize oxygen contamination. The furnace was then heated to the reaction temperature in 880 °C at 20 °C/min and was kept for 2 h. During synthetic process, Ar was flowing at 200 sccm and the pressure was maintained at atmospheric pressure (760 torr). The vapor-phase reactants transported by the Ar carrier gas condensed onto the substrate. After the reaction was finished, the quartz tube was cooled to the room temperature at 20 °C/min and then substrate was taken out. The substrate looks purple stains, indicating TiO_2 nanowires were synthesized on substrate.

The growth of TiO_2 nanowires is governed by two processes including i) Ti (g) + O_2 (g) → TiO_2 (s) and ii) TiO (g) + 0.5 O_2 (g) → TiO_2 (s).[29] As a titanium source, Ti(g) and TiO(g) are generated from the Ti layer deposited on substrate and the loaded TiO powder, respectively. Although we made the quartz tube was evacuated and flushed several times to minimize oxygen contamination before the experiment, a small amount of oxygen still remains in quartz tube,

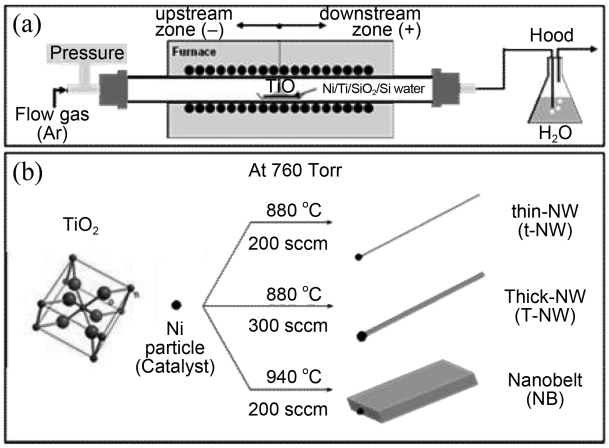

Figure 1. (a) Schematic diagram of the furnace used for the synthesis of TiO_2 nanostructures. (b) Different morphologies of TiO_2 nanostructures controlled by the Ar gas flow rate and growth temperature: t-NW, thin-NW; T-NW, Thick-NW; NB, Nanobelt.

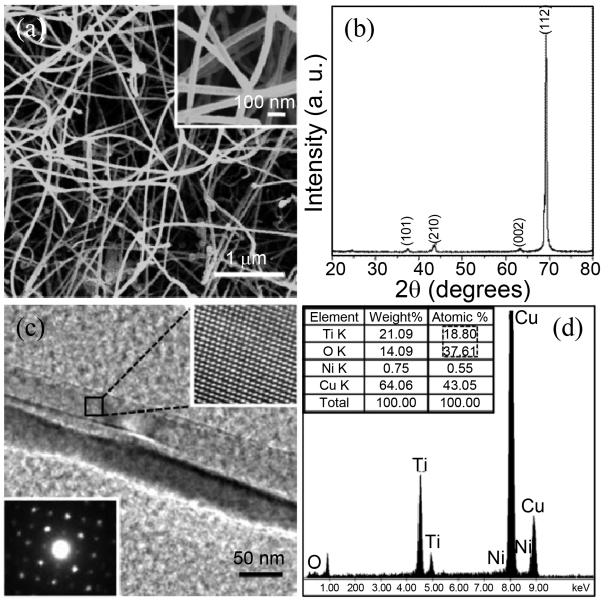

Figure 2. (a) Representative SEM image and (b) XRD pattern of rutile TiO_2 nanowires, as grown on a Ni/Ti/SiO_2/Si substrate; inset of (a) shows the high-magnification SEM image of TiO_2 nanowires. Scale bar is 100 nm. (c) Low-magnification TEM image of a TiO_2 nanowires. Scale bar is 50 nm. Inset of (c): top, HRTEM image taken from the area designated in (c); bottom, SAED pattern indexed for rutile TiO_2 crystalline. (d) EDX spectroscopy data of TiO_2 nanowires. Inset table of (d) shows the quantitative atomic ratio of Ti:O is 1:2.

which may come from the leakage of the reaction chamber and residual products in Ar carrier gas. This oxygen gas played an important role in the growth of TiO_2 nanowires.

As shown in Figure 1(b), various morphologies of single crystalline TiO_2 nano-structures are realized by controlling the growth temperature and flow rate of carrier gas. Reaching to growth temperature, Ni layer deposited on Ti/SiO_2/Si substrate turns into the nano-sized liquid droplets as a metal catalyst. We characterized the morphology of TiO_2 nanowires using a scanning electron microscope (SEM) and confirmed their crystallinity by a transmission electron microscope (TEM) study. Figure 2(a) shows the representative SEM image of TiO_2 nanowires grown on the Ni/Ti/SiO_2/Si substrate which were synthesized at 880 °C with 200 sccm Ar for 2 h. The diameter of produced TiO_2 nanowires usually range from 25 to 50 nm and their length is up to tens of micrometers.

The XRD peaks of TiO_2 nanowire exhibit the tetragonal structure of rutile TiO_2 [space group: P42/mnm (No. 136) with lattice constants a = 4.5933 Å and 2.9592 Å (PDF#00-021-1276)] (Figure 2(b)). In Figure 2(c), TEM image and selective area electron diffraction (SAED) pattern obtained from TiO_2 nanowire confirm that TiO_2 nanowire is single-crystalline. The high-resolution TEM (HRTEM) image taken from the area designated on TiO_2 nanowire also shows clear lattice fringes. Figure 2(d) shows the energy-dispersive X-ray (EDX) spectroscopy that confirms the 1:2 ratios of Ti and O atoms in the TiO_2 nanowire.

Thickness Control by Changing Gas Flow Rate. We

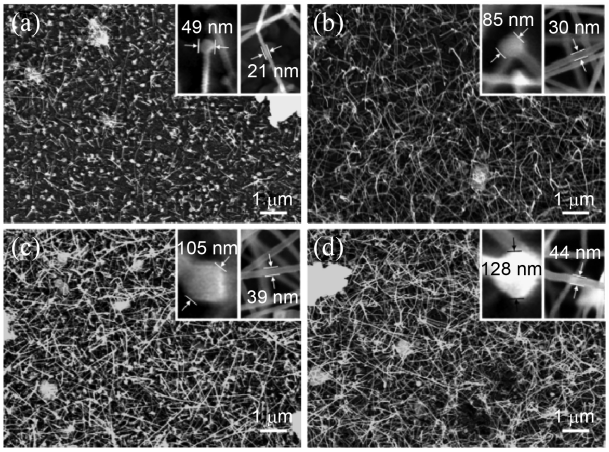

Figure 3. SEM images of TiO_2 nano-structures synthesized at different Ar gas flow rate, as grown on a Ni/Ti/SiO_2/Si substrate. To investigate the influence of carrier gas flow rate, the nanostructures were synthesized at (a) 100 sccm, (b) 150 sccm, (c) 200 sccm, and (d) 300 sccm for 2 h. Scale bar is 1 μm. Insets are high magnification SEM images of TiO_2 nanowires; left, the alloy tip on the top of TiO_2 nanowires; right, the diameter of the TiO_2 nanowires.

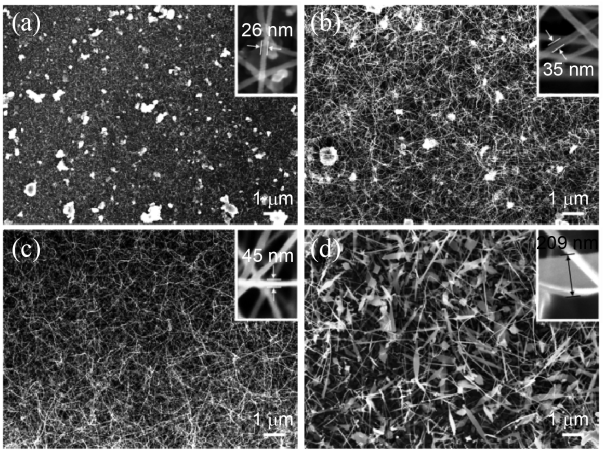

Figure 4. SEM images of TiO_2 nanostructures synthesized at different growth temperature, as grown on a Ni/Ti/SiO_2/Si substrate. To investigate the influence of growth temperature, the nanostructures were synthesized at (a) 860 °C, (b) 880 °C, (c) 900 °C, and (d) 940 °C for 2 h. Scale bar is 1 μm. Insets are high magnification SEM images of TiO_2 nanostructures.

conducted the synthesis of TiO_2 nanowires with varying flow rate of Ar gas to confirm whether or not the flow rate of carrier gas can influence the thickness of produced TiO_2 nanowires. Figure 3 shows the SEM images of TiO_2 nanowires at 880 °C with different flow rate of Ar gas for 2 h; (a) 100, (b) 150, (c) 200, and (d) 300 sccm. At the low gas flow rate, the density of produced TiO_2 nanowires looks low and their length and diameter are relatively short and thin (15-25 nm), respectively, although there are a little of TiO_2 thin nanowires with long length (Figure 3(a)). At the 150 sccm of Ar gas flow rate (Figure 3(b)), the TiO_2 nanowires have high density and longer length than the TiO_2 nanowires grown at 100 sccm while they have thin diameter such as 20-35 nm. Figure 3(c) shows a slight increasing of density and diameter of TiO_2 nanowires which have 25-40 nm diameters grown at 200 sccm. At the high gas flow rate, TiO_2 nanowires were synthesized with high density and thick diameter which is 40-55 nm (Figure 3, right of inset).

By increasing Ar gas flow rate, TiO_2 thick nanowires were mainly obtained with high density. To investigate the change in the thickness of TiO_2 nanowires caused by different flow rate of carrier gas, it is essential to study their growth mechanism. According to previous research, the growth of TiO_2 nanowires was processed by vapor-liquid-solid (VLS) mechanism, including that the vapor-phase reactant carried by carrier gas dissolves in the liquid Ni catalysts and then TiO_2 nanowires are formed by crystal precipitation through the supersaturation of TiO_2 components in liquid Ni catalysts. The nanowire produced by VLS mechanism has an alloy tip which is formed while the precursor dissolves into the catalyst. Compared with low gas flow rate at constant pressure (Atmospheric pressure; 760 torr), high gas flow rate causes large amount of vapor-phase reactant to dissolve in Ni catalysts due to a relatively fast carrying speed even though the equal reaction time. As shown in left insets of Figure 3, the TiO_2 nanowires grown at the high gas flow rate have a bigger alloy tip than the TiO_2 nanowires grown at low gas flow. Based on the fact that the diameter of TiO_2 nanowires depends on the size of the ally tip, it is reasonable that thicker TiO_2 nanowires are obtained with high density as increasing the gas flow rate. With these results, we believe that high gas flow rate can accelerate the growth kinetics of TiO_2 nanowires.

Morphology Control by Changing Growth Temperature. We synthesized the TiO_2 nanowires at different growth temperature in order to investigate the change of morphology caused by increasing growth temperature. Figure 4 shows the SEM images of TiO_2 nanowires produced at different growth temperature with 200 sccm of gas flow rate for 2 h; (a) 860 °C, (b) 880 °C, (c) 900 °C, and (d) 940 °C. At the low growth temperature, the density of produced TiO_2 nanowires looks low and their length and diameter are relatively short and thin (15-30 nm), respectively (Figure 4(a)). Upon shifting the growth temperature from 860 °C to 880 °C, and 900 °C, the diameter of produced TiO_2 nanowires gradually increased from 15-30 to 25-40, and 35-50 nm, as shown in Figure 4, indicating that the thickness of TiO_2 nanowires gradually increased as increasing growth temperature. With this result, the TiO_2 nanowires grown at 940 °C was produced to TiO_2 nanobelts with wide range of diameter such as 40-210 nm, as shown in Figure 4(d). Furthermore, TiO_2 nanobelts whose thickness usually ranges from tens of micrometers to several hundred micrometers are even synthesized.

By increasing growth temperature, we can synthesize not only the TiO_2 thick nanowires but also the TiO_2 nanobelts. In order to understand the morphology change influenced by growth temperature, we should consider the synthetic mechanism of TiO_2 nanowires. As above mentioned, it is known that the TiO_2 nanowires were synthesized by VLS

mechanism. However, during the reaction, the high growth temperature at constant pressure (Atmospheric pressure; 760 torr) makes more vapor-phase reactant than low reaction temperature. Because of high temperature and large amounts of vapor-phase reactant around the substrate whose site take places the synthetic process for formation of TiO_2 nanowires, there occur not only VLS mechanism but also VS mechanism including that vapor-phase reactant directly dissolves in formed solid nanostructure (i.e. TiO_2 nanowire) which was made by VLS mechanism. With this reason, VS mechanism can accelerate lateral growth of TiO_2 nanowires. As a result, TiO_2 nanobelts were synthesized at high growth temperature.

Conclusion

By changing reaction conditions such as gas flow rate and growth temperature, the various morphologies of high single crystalline rutile TiO_2 nanostructures such as thin-nanowires, thick-nanowires and nanobelts were synthesized. We also confirm the high single crystalline TiO_2 nanowires using SEM, XRD, TEM and EDX. The TiO_2 nanowires grown at high gas flow rate are highly dense and thick, because large amount of reactants can dissolve in the Ni catalysts with high carrying speed. With this result, the growth kinetics of TiO_2 nanowires can be accelerated and thicker TiO_2 nanowires is obtained. At high growth temperature, the TiO_2 nanobelts were usually obtained. Considering the high temperature and large amounts of vapor-phase reactant around the substrate, crystal growth was governed by VS mechanism as well as VLS mechanism, accelerating lateral growth TiO_2 nanowires. We believe that various morphologies of TiO_2 nano-structures should be useful for adjusting the properties of TiO_2 nanowires such as optical and electrical properties.

Acknowledgments. We are grateful to Prof. Won Il Park and Dong Hyun Lee for assistance with preparation of metal-catalyzed substrates using thermal evaporation. And, we thank Dr. Sang-ho Lee for helpful discussions. This Research was supported by the Sookmyung Women's University Research Grants 2009.

References

1. Hahn, R.; Schmidt-Stein, F.; Salonen, J.; Thiemann, S.; Song, Y. Y.; Kunze, J.; Lehto, V. P.; Schmuki, P. *Angew. Chem. Int. Ed.* **2009**, *48*, 1.
2. Boercker, J. A.; Enache-Pommer, E.; Aydil, E. S. *Nanotechnology* **2008**, *19*, 095604.
3. Cao, B.; Yao, W.; Wang, C.; Ma, X.; Feng, X.; Lu, X. *Materials Letters* **2010**, *64*, 1819.
4. Shi, J.; Sun, C.; Starr, M. B.; Wang, X. *Nano Lett.* **2011**, *11*, 624.
5. Wang, J.; Sun, J.; Bian, X. *Materials Science and Engineering A* **2004**, *379*, 7.
6. Nuansing, W.; Ninmuang, S.; Jarernboon, W.; Maensiri, S.; Seraphin, S. *Materials Science and Engineering B* **2006**, *131*, 147.
7. Pijanowska, D. G.; Sprenkels, A. J.; van den Linden, H.; Olthuis, W.; Bergveld, P.; van *den Berg, A. Sensors and Actuators B* **2004**, *103*, 350.
8. Shiraishi, Y.; Sugano, Y.; Tanaka, S.; Hirai, T. *Angew. Chem. Int. Ed*. **2010**, *49*, 1656.
9. Awazu, K.; Fujimaki, M.; Rockstuhl, C.; Tominaga, J.; Murakami, H.; Ohki, Y.; Yoshida, N.; Watanabe, T. *J. Am. Chem. Soc.* **2008**, *130*, 1676.
10. Qiu, Y.; Chen, W.; Yang, S. *Angew. Chem. Int. Ed*. **2010**, *49*, 3675.
11. Woolerton, T. W.; Sheard, S.; Reisner, E.; Pierce, E.; Ragsdale, S. W.; Armstrong, F. A. *J. Am. Chem. Soc.* **2010**, *132*, 2132.
12. Park, J. H.; Kim, S. W.; Bard, A. J. *Nano Lett.* **2006**, *6*, 24.
13. Pang, C. L.; Lindsay, R.; Thornton, G. *Chem. Soc. Rev.* **2008**, *37*, 2328.
14. Mao, S. S.; Chen, X. *Int. J. Energy Res.* **2007**, *31*, 619.
15. Mao, S. S.; Chen, X. *Int. J. Energy Res*. **2007**, *31*, 619.
16. Fabregat-Santiago, F.; Barea, E. M.; Bisquert, J.; Mor, G. K.; Shankar, K.; Grimes, C. A. *J. Am. Chem. Soc.* **2008**, *130*, 11312.
17. Liu, B.; Aydil, E. S. *J. Am. Chem. Soc.* **2009**, *131*, 3985.
18. Kolmakov, A.; Moskovits, M. *Annu. Rev. Mater. Res.* **2004**, *34*, 151.
19. Miao, Z.; Xu, D.; Ouyang, J.; Guo, G.; Zhao, X.; Tang, Y. *Nano Lett.* **2002**, *2*, 717.
20. Wei, M,; Qi, Z. M.; Ichihara, M.; Hirabayashi, M.; Honma, I.; Zhou, H. *Journal of Crystal Growth* **2006**, *296*, 1.
21. Lee, Y. H.; Yoo, J. M.; Park, D. H. *Applied Physics Letters* **2005**, *86*, 033110.
22. Kominami, H.; Ishii, Y.; Kohno, M.; Konishia, S.; Kera, Y.; Ohtanic, B. *Catalysis Letters* **2003**, *91*, 1.
23. Amin, S. S.; Li, S. Y.; Wu, X.; Ding, W.; Xu, T. T. *Nanoscale Res. Lett.* **2010**, *5*, 338.
24. Park, J. B.; Ryu, Y.; Kim, H. S.; Yu, C. H. *Nanotechnology* **2009**, *20*, 105608.
25. Daothong, S.; Songmee, N.; Thongtem, S.; Singjai, P. *Scripta Materialia* **2007**, *57*, 567.
26. Wu, J. J.; Yu, C. C. *J. Phys. Chem. B* **2004**, *108*, 3377.
27. Chen, C. A.; Chen, Y. M.; Korotcov, A.; Huang, Y. S.; Tsai, D. S.; Tiong, K. K. *Nanotechnology* **2008**, *19*, 075611.
28. Yu, J.; Chen, Y.; Glushenkov, A. M. *Crystal Growth & Design* **2009**, *9*, 1240.
29. Baik, J. M.; Kim, M. H.; Larson, C.; Chen, X.; Guo, S.; Wodtke, A. M.; Moskovits, M. *Applied Physics Letters* **2008**, *92*, 242111.
30. Amin, S. S.; Nicholls, A. W.; Xu, T. T. *Nanotechnology* **2007**, *18*, 445609.
31. Lee, J. S.; Brittman, S.; Yu, D.; Park, H. K. *J. Am. Chem. Soc.* **2008**, *130*, 6252.
32. Peng, H.; Meister, S.; Chan, C. K.; Zhang, X. F.; Cui, Y. *Nano Lett.* **2007**, *7*, 199.